

# 5

---

## *Colloidal PbS quantum dots on GaAs: Optical properties and Urbach tail slope tuning*

---

B Ullrich<sup>1,2</sup>, A K Singh<sup>1</sup>, J S Wang<sup>3</sup>, H Xi<sup>4</sup>

<sup>1</sup>Instituto de Ciencias Físicas, Universidad Nacional Autónoma de México, Cuernavaca, Morelos 62210, Mexico

<sup>2</sup>Ullrich Photonics LLC, Wayne, OH 43466, USA

<sup>3</sup>Air Force Research Laboratory, Materials & Manufacturing Directorate, Wright Patterson AFB, OH 45433-7707, USA

<sup>4</sup>Department of Physics and Astronomy, Bowling Green State University, Bowling Green, OH 43403-0209, USA

### Outline:

Introduction .....	134
Sample preparation and photoluminescence of the colloidal PbS QDs .....	134
Optical absorbance of strongly confined PbS quantum dots .....	139
Urbach tail slope tuning and band gap engineering of GaAs by the influence of deposited PbS QDs .....	142
Conclusions .....	145
Acknowledgement .....	146
References .....	146

## Introduction

Emphasizing the importance of this material, the III-V compound semiconductor Gallium Arsenide (GaAs) and related compounds revolutionized in the mid-1980s the commercial mass-market industry by being the key component for integrated laser circuits, which paved the way for high-dense digital information carriers, such as compact discs. This period in time revealed one of the most impressive technology revolutions initiated by the control of material properties on an atomic level, enabling the formation of quantum wells and superlattices, i.e., the superposition of quantizing periodic potentials with widths typically in the  $\sim 10$  nm ranges superimposed to the natural potential pattern of the solid host. Most of the groundbreaking work was done by molecular beam epitaxy (MBE) [1,2], which allows the epitaxial growth of abrupt two-dimensional selectively doped layer sequences [3,4]. The built-in potential shapes, which confine the electron and hole wave functions, may vary being for example rectangular or triangular. Due to the high-precision periodicity of the potentials, the sub-band energy transitions of these superlattices can be precisely described with the Kronig-Penney model [5].

Almost coincidental with the emerging maturity of MBE produced devices, in particular the optical properties of semiconducting “quantum crystals” or “quantum dots” (hereafter QDs) in the 2 to 50 nm size regime moved to the center of increasing research interests [6]. In a way, QDs can be understood as free standing energy confinement potentials for charge carriers (not necessarily electronically linked to the host) and, therefore, as discussed below, fairly regularly arranged QD ensembles are expected to reveal properties similar to superlattices, although the synthetic methods are entirely different and in many cases more cost effective. Among several preparation routes, which are summarized in ref. [7], the employment of colloidal wet solutions containing stabilizing agents in order to prevent the cluster-up of the QDs are attractive precursors for the self-assembled formation of colloidal QD arrays, which are investigated here.

While the aforementioned efforts focus on “single” materials (or combinations of closely related materials), the investigation of hetero-paired hybrids - for example the merger of organic with inorganic materials [8] - became a growing research topic during the last two decades because of the tremendous application potential in optoelectronics, photovoltaics, and bio-physics, to mention a few. In the current work, by presenting rarely or none studied phenomena such as photo-doping in QDs, absorbance of strongly confined QDs, and Debye temperature decrease due to matter size shrinking, we emphasize the optical properties of a “size-hybrid” by investigating colloidal Lead Sulfide (PbS) QDs deposited on the surface of industrially provided GaAs wafers, whereas the affect of the QDs on the GaAs absorption features, in particular the influence on the Urbach tail, is the new and so far not studied subject here-in.

## Sample preparation and photoluminescence of the colloidal PbS QDs

Oleic acid capped PbS QDs with sizes of between 2.0 nm and 4.7 nm have been investigated. The QDs are dispersed either with a supercritical fluid CO<sub>2</sub> method [9], a straightforward solvent deposition [10], and spin-coating (3000 rpm for 40 seconds) on semi-insulating GaAs (SI-GaAs) and for comparative purposes on glass. Table 5.1 displays the samples investigated.

**TABLE 5.1**

Parameters of the samples investigated

Sample	Substrate	Preparation method	QD size
A	GaAs	Solvent deposition	4.7±0.5 nm
B	GaAs	Critical CO <sub>2</sub>	2.0±0.4 nm
C	Glass	Critical CO <sub>2</sub>	2.7±0.4 nm
D	GaAs	Spin-coating	3.0±0.5 nm

Figure 5.1 shows the scanning electron microscopy (SEM) image of sample B revealing homogeneous surface coverage with a gap of 0.2-0.5 nm between the individual particles. For the ongoing discussion, it is important to point out that in a closed packed quantized array, as the one displayed in fig. 5.1, the sub-bands of the individual QDs show coupling because the charge carrier tunneling range ( $\Delta x$ ), which is expressed by,

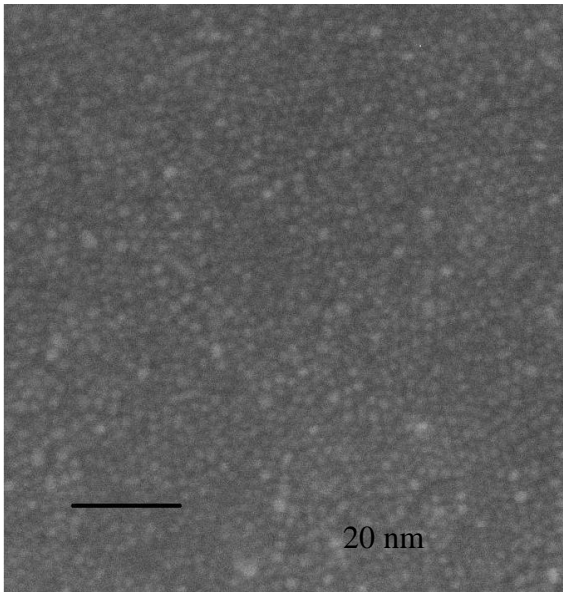
$$\Delta x = \frac{h}{4\pi\sqrt{2m_{e,h}^*E_{gs}}}, \quad (1)$$

overcomes or matches the separation of the QDs, where  $h$  is Planck's constant,  $m_{e,h}^*$  is the effective electron (or hole) mass, and  $E_{gs}$  is the QD ground state energy,

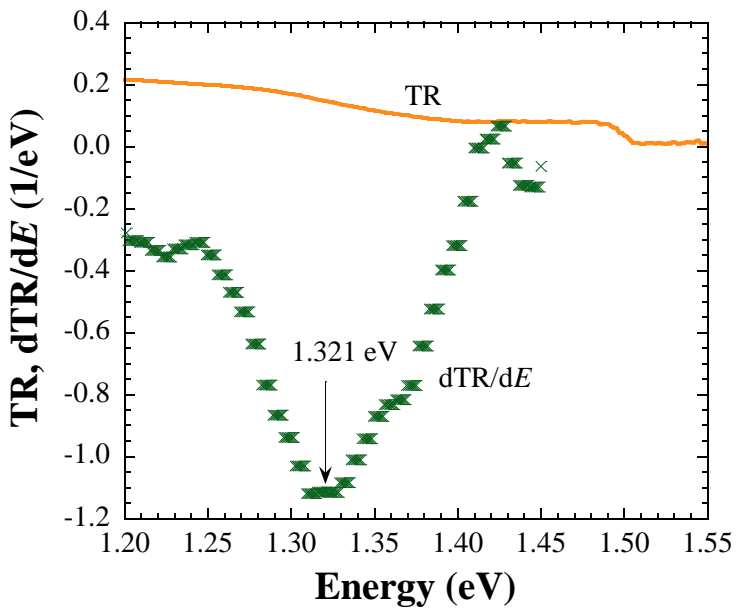
$$E_{gs} = \frac{E_g - E_{g,bulk}}{2}, \quad (2)$$

where  $E_g$  is the band gap energy of the QDs and  $E_{g,bulk}$  is the band gap energy of bulk PbS, whereas the symmetry of eq. (2) is caused by  $m_e \approx m_h = 0.08 \times m_0$  [10] with  $m_0$  being the free electron mass. Figure 5.2 shows the determination of  $E_g$  of sample B at 5 K employing transmittance (TR) spectroscopy. By plotting  $dTR/dE$  we locate  $E_g$  at 1.321 eV, resulting with  $E_{g,bulk} = 0.29$  eV in  $\Delta x = 0.5$  nm indeed matching or exceeding the inter QD spacing in fig. 5.1.

In order to measure the TR spectrum shown in fig. 5.2, the emission of the internal quartz lamp of a BOMEM Fourier transform infrared (FTIR) spectrometer was guided to the sample, which was mounted in an optical cryostat. The TR signal was detected with a nitrogen cooled Indium Gallium Arsenide (InGaAs) detector attached to the BOMEM. The principle of FTIR and its advantages with respect to dispersive techniques have been discussed elsewhere [11,12].

**FIGURE 5.1**

SEM image (taken with an acceleration voltage of 10 kV and a working distance of about 4.5 mm) of a typical PbS QD self-assembled dispersion (sample B). The size of the QDs is  $2.0 \pm 0.4$  nm

**FIGURE 5.2**

TR spectrum and  $dTR/dE$  of sample B at 5 K. The sample starts to transmit at the band gap of GaAs ( $\sim 1.5$  eV). The band gap value  $E_g$  of the QDs is found to be at 1.321 eV

The perhaps most important property, specifically with regard to technological applications, is the photoluminescence (PL) of the QDs. The PL was measured in the same way as the TR spectra with the difference being the optical excitation was provided by the 532 nm continuous wave (cw) emission of a solid state laser. Figure 5.3 reveals the PL spectra of sample B for various impinging laser intensities ( $I_{ex}$ ) at 5 K. A blue shift of the spectra takes place. It is clearly of importance to check whether the shift is caused by dynamic band filling (Burstein-Moss shift) [13]. The latter phenomenon has been investigated in CdS QDs in the pioneering days of QD research [14], but was never clarified beyond doubt. For bulk semiconductors, the theoretically expected trend of the PL peak as a function of the photo-generated electron-hole pairs ( $n$ ), which are excited with the laser irradiation, is expressed by,

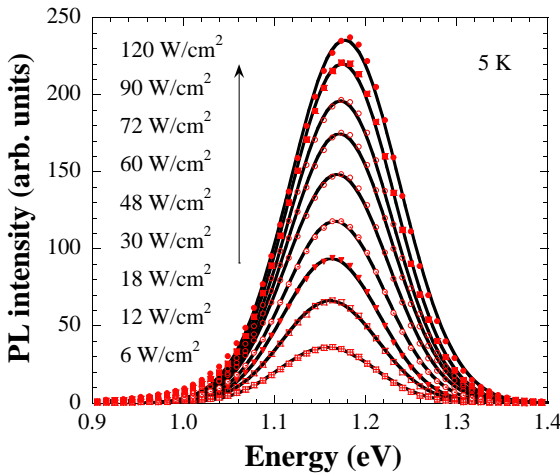
$$E_{PL}(n) = E_{PL0} + \Delta E(n) \tag{3}$$

and [7],

$$\Delta E(n) = 0.97 \times n^{2/3} \{h^2 / (8\mu)\}, \tag{4}$$

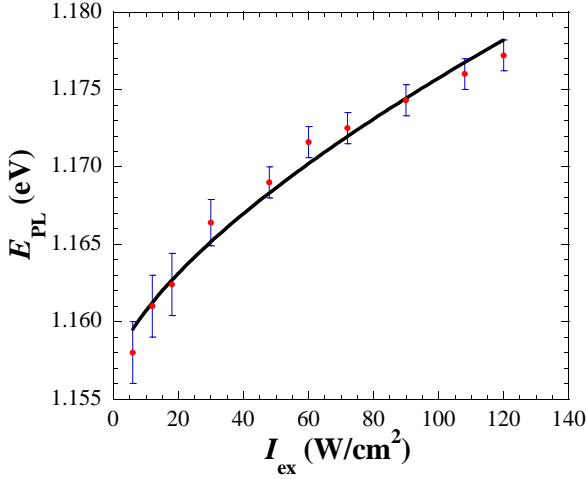
where  $E_{PL}$  and  $E_{PL0}$  is the PL peak energy under laser irradiation and without influence of band filling, respectively,  $\Delta E$  is the photo-induced energy shift, and  $\mu = 0.04 \times m_0$  is the reduced effective mass at 5 K [10], favoring band filling due to its small value. The link between  $n$  and the impinging laser beam is given by [15],  $n = \alpha_{PL} \tau_r I_{ex} / h \nu_{ex}$ , where  $\tau_r$  is the radiative lifetime,  $\alpha_{PL}$  is the absorption coefficient probed during the PL experiments, and  $h \nu_{ex} = 2.33$  eV is the energy of the impinging exciting laser beam. Hence, the equation for the dynamic Burstein-Moss shift becomes,

$$E_{PL}(I_{ex}) = E_{PL0} + 0.97 \times [\alpha_{PL} \tau_r I_{ex} / h \nu_{ex}]^{2/3} \{h^2 / (8\mu)\}. \tag{5}$$



**FIGURE 5.3**

PL spectra of sample B measured at various  $I_{ex}$ . The symbols are the measured data and the solid lines Gaussian fits. With increasing  $I_{ex}$  the PL spectra shift towards higher energies

**FIGURE 5.4**

The symbols represent the  $E_{\text{PL}}$  position in fig. 5.3 vs.  $I_{\text{ex}}$ . The solid line shows the fit with eq. (5)

The line in fig. 5.4, which displays  $E_{\text{PL}}$  vs.  $I_{\text{ex}}$ , represent the fit using eq. (5) showing excellent agreement with the measurements ( $\chi^2=0.99$ ), while  $E_{\text{PL}0}$  and  $\alpha_{\text{PL}}\tau_r$  are found to be 1.157 eV and  $3.5\times 10^{-4}$  s/cm. We should stress that the data trend in fig. 5.4 validates our qualitative interpretations in previous papers [15,16]. Nevertheless, we check whether the experimental conditions permit the generation of at least one electron-hole pair per QDs ( $n_{\text{QD}}$ ) in order to make band filling realistic. Defining the QD absorption cross section with  $\sigma=\alpha_i V_{\text{QD}}$  [17], where  $\alpha_i$  is the intrinsic absorption coefficient of an individual QD (not necessarily matching  $\alpha_{\text{PL}}$ ) and  $V_{\text{QD}}$  is the QD's spherical volume ( $4\times 10^{-21}$  cm<sup>3</sup>), we write for  $n_{\text{QD}}$ ,

$$n_{\text{QD}}=I_{\text{ex}}\tau_r\sigma/h\nu_{\text{ex}}. \quad (6)$$

With  $\tau_r\sim 10$   $\mu\text{s}$  [18] and  $\alpha_i=1\times 10^5$  cm<sup>-1</sup> [17], we calculate  $n_{\text{QD}}=1.3$  at  $I_{\text{ex}}=120$  W/cm<sup>2</sup>. Consequently, the result confirms the realization of the Burstein-Moss shift in the QD ensemble.

In ref. 16, by investigating the PL of colloidal 4.7 nm QDs on glass, it was observed that the blue shift of the PL is considerably temperature dependent and almost vanishing at room temperature. The reason for this behaviour is that band filling scales with the inverse of the effective mass. The latter grows with temperature, and, as a consequence, many body effects start to compensate or probably even capsizing the Burstein-Moss shift at higher temperatures [16]. Work on the temperature dependence of the effective mass in QDs is scarce - smaller QDs are expected to show a more pronounced temperature dependence of the effective mass [19]. While all of our results at cryogenic temperatures reveal a blue shift, the PL spectra in fig. 5.5 of sample C (QD size 2.7 nm) measured at room temperature (RT) with the identical experimental setup used in ref. 16 show a red shift, pointing to band gap shrinkage due to many body effects [2,16], and therefore, to a stronger growth of the effective mass in extremely confined QDs. To the best of our knowledge, the result in fig. 5.5 represents the first manifestation of many body effects in colloidal QDs.

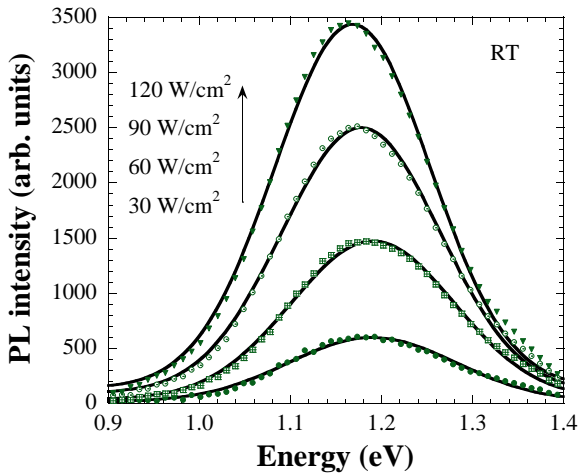


**FIGURE 5.5**

PL spectra of sample C for selected  $I_{\text{ex}}$  values at RT. The spectra display a red shift due to many body effects. The solid lines are Gaussian fits

Finally, it is worthwhile to stress why eq. (4), which is derived for three-dimensional semiconductors with parabolic bands, describes the events in fig. 5.4. The cause is the tunneling range of the excited carriers pointed out by eq. (1), allowing the formation of an electronically coupled QD array – in a manner similar to the potential coupling in superlattices – ruled by theories based on three-dimensions.

## Optical absorbance of strongly confined PbS quantum dots

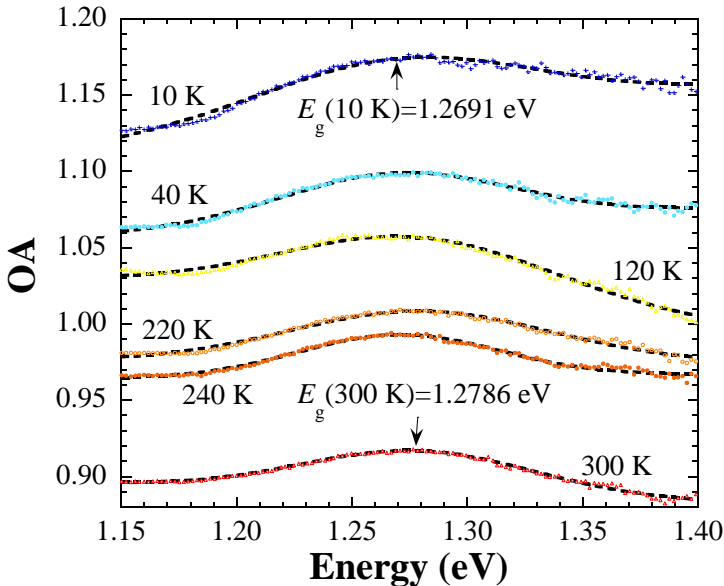
The energy of the lowest optical absorbance (OA) transition of QDs has been intensively studied in a wide variety of QDs under myriad experimental conditions in the last 25 years [20]. Colloids of PbS QDs attracted particular attention [21] due to the beneficial intrinsic material properties, the relative ease and flexibility of sample fabrication [9], and the potential for integration in optoelectronic GaAs based device structures [22]. Specifically, with regard to the latter application, investigations of thermo-optical properties of PbS QDs with diameters below 3 nm is crucial for the development of effective light emitters because the recombination coefficient of semiconductors scales with  $E_g^2$  [23]. However, apart from our work [24], we did not find literature showing the variations of the OA spectra with temperature of lead-salt QDs with a diameter below 3 nm. Two reasons can be attributed for the data vacancy. First, it is difficult to get reliable data for such small, strongly confined QDs owing to their weak OA features, and second, the difficulty in pinpointing the fundamental transition because of the intrinsic broadening of the OA peak with shrinking QD diameters [25]. Notwithstanding, here we report the OA temperature dependence of colloidal PbS QDs with size smaller than 3 nm. The results reveal (a) vibronic mode damping as a consequence of increasing quantum confinement and (b) the compatibility of Fan's classical theory with strongly size-quantized matter.

Figure 5.6 shows the OA spectra of sample C at various temperatures. The symbols represent the measurements and the dotted lines Gaussian fits ( $\chi^2 \geq 0.988$ ) incorporating a linear offset, which is caused by the light scatter at the ligands. The peak of the OA spectra defines  $E_g$ , which, towards

cryogenic temperatures, reveals a subtle red shift. The energy of  $\sim 1.28$  eV agrees very well with the expected  $E_g$  at RT of colloidal 3 nm PbS QDs [21]. The symbols along the broken line (a) in fig. 5.7 shows  $E_g$  vs. temperature [ $E_g(T)$ ] localized with Gaussian fits as the ones presented in fig. 5.6, while the line itself is a linear fit ( $\chi^2=0.774$ ) with a temperature coefficient of  $dE_g/dT=40$   $\mu\text{eV/K}$ . The trend differs considerably from the nonlinear  $E_g(T)$  behavior for colloidal 4.7 nm QDs. The experimental data, which are taken from ref. [10], are represented by the symbols along the solid curve (b). The latter represents a fit ( $\chi^2=0.998$ ) with Fan's equation [26],

$$E_g(T)=E_g(0)+A/\{\exp(\langle E_p \rangle/kT)-1\}, \quad (7)$$

where,  $E_g(0)=0.9223$  eV is the low limit of the band gap for temperatures approaching 0 K,  $A=23.4$  meV is the Fan parameter, which depends on the microscopic material properties and is considered widely temperature invariant,  $\langle E_p \rangle=15.5$  meV is the average phonon energy responsible for the band gap variation, and  $k=8.62 \times 10^{-5}$  eV/K is the Boltzmann constant. Bearing in mind that  $A \propto \langle E_p \rangle^{1/2}$  [10], we note that for  $\langle E_p \rangle \rightarrow 0$  eV, eq. (7) gives the temperature invariant result  $E_g(T)=E_g(0)=\text{constant}$ .



**FIGURE 5.6**

OA spectra of sample C at selected temperatures. The symbols represent the measurements and the broken line Gaussian fits with a linear offset

Further analysis of the theoretical background regarding eq. (7) reveals that  $A$ , which is also called self-energy, is identical with the PL Stokes shift ( $\Delta_{\text{Stokes}}$ ) [27]. In a former work [10], we pointed out that  $\Delta_{\text{Stokes}}$  depends on the temperature. As a consequence,  $A$  cannot be considered to be temperature invariant and the  $A$  value found with the fit in fig. 5.7 represents an average value like  $\langle E_p \rangle$ , which varies with temperature as well. Hence,  $A$  ought to be replaced by  $\langle A \rangle$  in eq. (7), whilst the connection between the Fan theory and  $\Delta_{\text{Stokes}}$  require more theoretical attention. Currently, based on the findings in refs. [10] and [27], we work on a generally valid theory defining the intrinsic Stokes shift in semiconductors.

The classical theory of Fan describes  $E_g(T)$  in terms of electron-phonon interactions in bulk semiconductors. Looking at curve (b) in fig. 5.7, at temperatures below  $\sim 50$  K, due to the damping of the acoustic phonons, only relatively subtle changes of  $E_g$  take place ( $\sim 40$   $\mu\text{eV/K}$ ), while for elevated temperatures the broader phonon spectrum intensifies the dependence of  $E_g$  on temperature changes, resulting in  $dE_g/dT=117$   $\mu\text{eV/K}$ . The overall appearance of  $E_g(T)$  is therefore nonlinear. Consequently, curve (b) in fig. 5.7 qualitatively represents the behavior of a bulk semiconductor. The linear trend of curve (a), however, clearly deviates from the typical “Fan-like” characteristic. Nevertheless, as demonstrated by the positively curved solid line in fig. 5.8, which shows  $E_g(T)$  in the cryogenic region, the data can be fitted with eq. (7) resulting in  $\chi^2=0.834$  – clearly improved with respect to the linear fit represented by the broken line. The increase in the fit goodness by the use of Fan’s expression reflects the subtle trend of  $dE_g/dT$  to flatten below  $\sim 30$  K. The uncertainties of the OA peak positions refer to measured fluctuations (found by repetitive measurements) rather than to an error caused by the fitting methods applied. The fit parameters are:  $E_g(0)=1.2667$  eV,  $A=0.9$  meV, and  $\langle E_p \rangle=1.98$  meV - note the reduction of about one order of magnitude of  $A$  and  $\langle E_p \rangle$  with respect to the values found for the 4.7 nm QDs. This apparent shrinkage of  $\langle E_p \rangle$  causes a decrease of the Debye temperature, which is given by  $\langle E_p \rangle/k$  [10], from 180 K to 23 K, pointing to the dilution of the vibrational mode diversity in strongly confined matter.

In order to comprehend the qualitative difference between shapes (a) and (b) in fig. 5.7, the number of atoms forming the QDs is essential. The amount of atoms is given by  $(4\pi/3) \times (d/a)^3$  [21] where  $d$  is the QD diameter and  $a$  is the lattice constant of PbS ( $5.936 \times 10^{-10}$  m). For 2.7 nm and 4.7 nm, we find 394 and 2079 atoms within the QDs. Specifically the result for the 2.7 nm QDs (sample C) is clearly below the required atom number of  $\sim 10^4$ , which is necessary to form crystallites possessing fully developed bulk properties [28]. As a consequence, the low number of atoms drastically limits the vibronic occurrences in sample C. Meanwhile, we pointed out that phonons vanish in PbS QDs limited to 90 atoms [24].

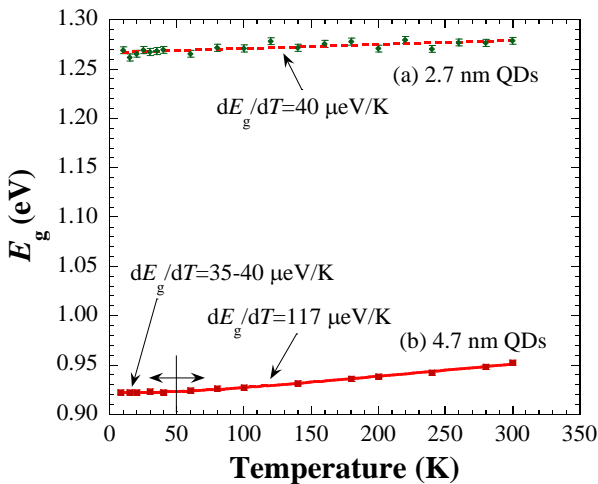


**FIGURE 5.7**

The measured  $E_g(T)$  represented by the symbols for QDs of (a) 2.7 nm (sample C) and (b) 4.7 nm size [10]. The trend of (a) is fitted with a straight line resulting in a constant  $dE_g/dT=40$   $\mu\text{eV/K}$  over the entire temperature range. The nonlinear  $E_g(T)$  of (b) is fitted with Fan’s expression (7) and shows two slope regions. Below 50 K,  $dE_g/dT=35-40$   $\mu\text{eV/K}$  and above 50 K  $dE_g/dT=117$   $\mu\text{eV/K}$ . The error bars of trend (b) coincide with the symbol size

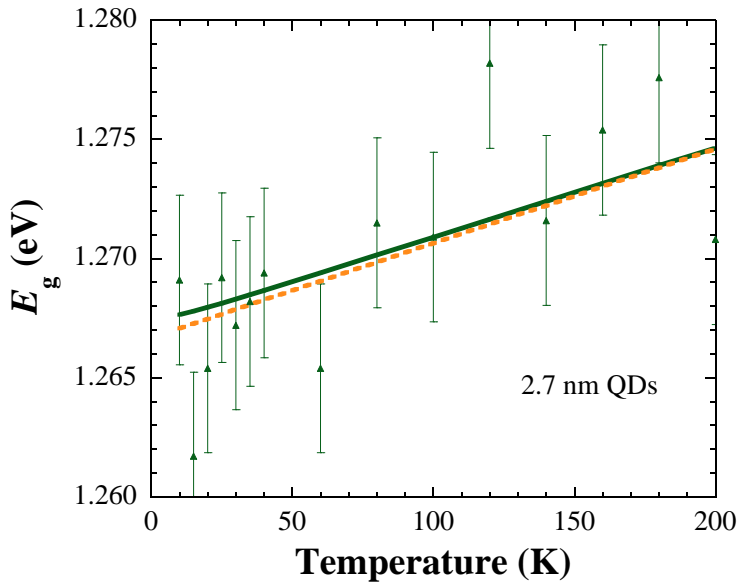


**FIGURE 5.8**

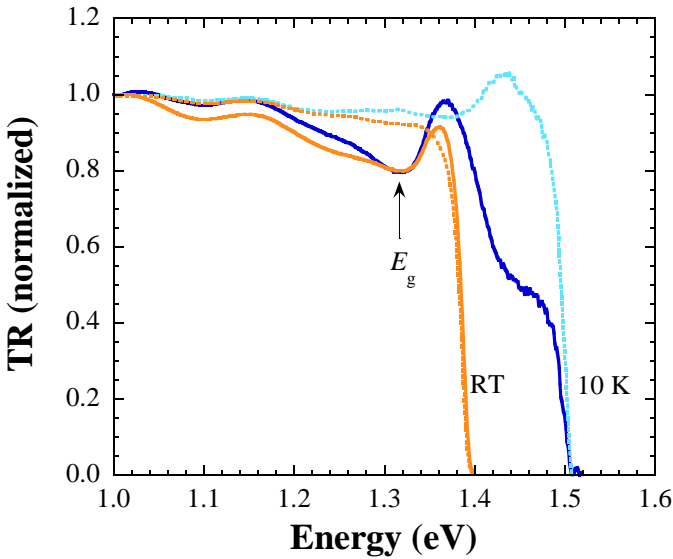
Detailed comparison of the linear fit (broken line, which is identical with the one in fig. 5.7) and the fit using Fan's formula (solid line). The Fan fit clearly deviates from the linear fit for decreasing temperatures because of the replication of the more flat  $E_g$  variations at cryogenic temperatures

## Urbach tail slope tuning and band gap engineering of GaAs by the influence of deposited PbS QDs

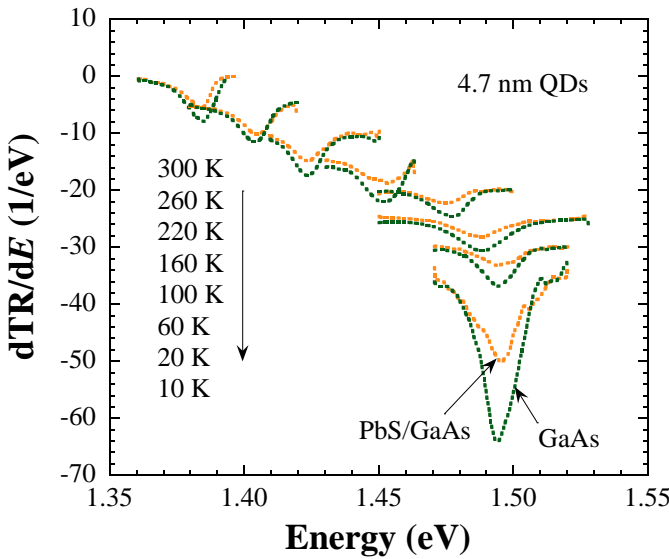
Here, we pursue an uncommon task, i.e., the investigation of the influence of the deposited QDs on the absorption of the substrate rather than the properties of the QDs themselves. To the best of our knowledge, such studies have not been performed and are motivated by an earlier work of us on the PL properties of PbS QDs dispersed on Si-GaAs [22]. In this work it was recognized that deposition of PbS QDs on GaAs enhances the GaAs emission and evoked additional luminescent transitions. The observations have been explained by charge transfer from the QDs to the GaAs substrate.

Figure 5.9 shows the comparison of TR spectra of Si-GaAs wafers and sample B measured at cryogenic temperatures and RT. The measurements have been carried out at a different spot than the TR experiment shown in fig. 5.2 and show more pronounced features. The superposition of the QD absorption with the GaAs absorption clearly alters the TR of the samples causing a signal modulation in the transmissive range of the GaAs substrate, according to the quantized energy transitions. The results reveal that  $E_g \sim 1.32$  eV do not shift with temperature - as expected for PbS QDs with size of 2.0 nm [24,29]. The origin of local TR decrease around 1.42 eV at 10 K, which does not appear in the TR in fig. 5.2, is unclear. It is probably caused by the random absorption of the smaller QDs in the illuminated ensemble. At this point, we focus on the slope of the TR edge in the vicinity of the TR threshold at the GaAs band gap, i.e., the steepness of the Urbach tail ( $dTR/dE$ ). A comprehensive study over the entire

temperature range was carried out with sample A. The result is shown in fig. 5.10, demonstrating that the maxima of the  $dTR/dE$  values of the bare GaAs wafer exceed the numbers of the PbS/GaAs sample over the entire temperature range of 10 K – 300 K. Figure 5.11 displays the difference ( $|\delta|$ ) between the individual  $dTR/dE$  values in fig. 5.10.



**FIGURE 5.9**  
TR spectra at 10 K and RT of SI-GaAs wafers (dotted lines) and sample B (solid lines)



**FIGURE 5.10**  
 $dTR/dE$  for selected temperatures for sample A. As indicated for 10 K, at all temperatures the  $dTR/dE$  value of the SI-GaAs wafer exceeds that of the PbS/GaAs sample. For clarity, the spectra, which possess Gaussian-like shape, are shifted

Discussing the outcomes displayed in figs. 5.10 and 5.11, i.e., the more pronounced Urbach tail in the PbS/GaAs sample, it is necessary to bear in mind the causes of the below-band gap absorption, which is attributed to transitions between band tails [7]. Such tails can originate from defects or impurities and scattering of charge carriers by phonons [13,30]. Hence, the observed results could be caused by adding recombination centers at the substrate surface below the GaAs band gap. It is known that the oleic acid ligands preferentially bind to lead atoms on the QD surface and leave the sulfur atoms unpassivated, which allows for possible hole traps [31]. Thus, it is conceivable that these traps take part in the recombination events of the GaAs wafers. As already mentioned, by investigating the PL of PbS/GaAs samples [22], we concluded that charge transfer from the QDs to the GaAs substrate takes place. These transferred carriers enhance the PL signal of the GaAs substrate. We do not think that transferred charge carriers, which in the previous work [22] have been excited with laser irradiation far above the QD and GaAs band gaps, play an essential role for the observations here, but resonant optical excitations at the GaAs band gap region. On the other hand, the trend of  $|\delta|$  in fig. 5.11 indicates the involvement of acoustic phonons in the results displayed in figs. 5.9 and 5.10: At elevated temperatures the absorption edge is equally blurred by thermal means resulting in a fairly constant  $|\delta|$  for the GaAs substrate and the PbS/GaAs sample, while at low temperatures the acoustic phonons are bleached causing the relative increase in  $|\delta|$ .

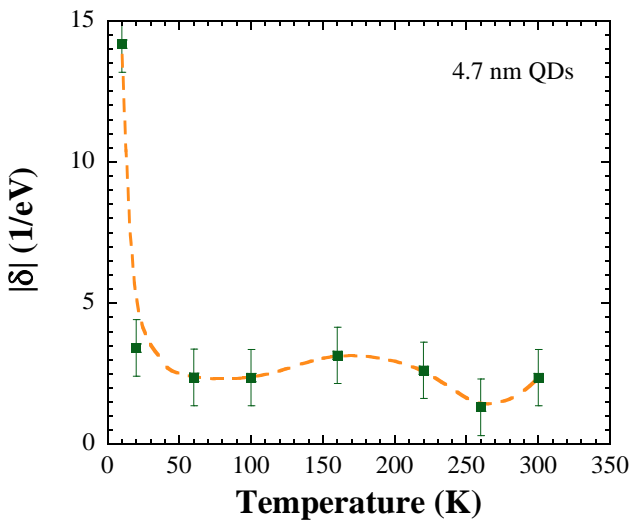


**FIGURE 5.11**

The absolute differences of the individual  $dTR/dE$  peak values in fig. 5.10. The broken line is a guide for the eye

Figure 5.12 shows the comparison of the RT  $dTR/dE$  spectra of sample B in fig. 5.9 to that of sample D. We note that sample D is the only one not measured with the BOMEM spectrometer, but with a Newport Cornerstone monochromator in conjunction with a 100 W halogen lamp. The TR signal was measured by a Silicon (Si) photodiode mounted behind the sample. We further emphasize that the smaller QDs (with  $E_g$  in the vicinity of the GaAs energy band gap) influence the Urbach tail in the opposite way. The presence of the QDs increases the steepness of the GaAs absorption edge. We believe that for samples B and D the superposition of the QD and GaAs TR spectra determines the slope of the Urbach tail rather than the formation of trap states.

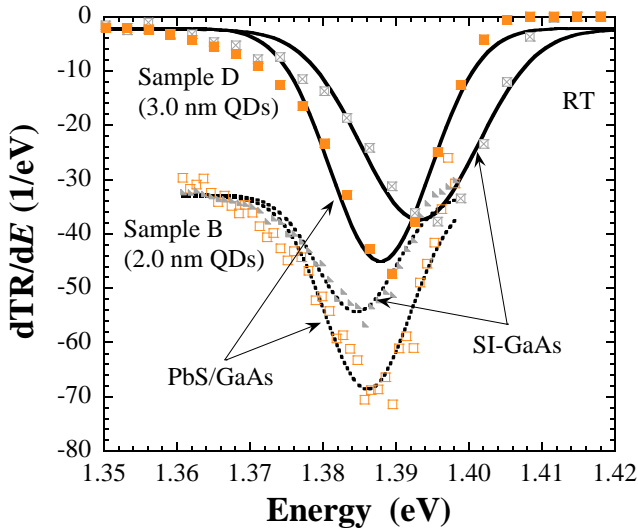


**FIGURE 5.12**

The symbols represent the experimental  $dTR/dE$  spectra of samples B and D and the dotted and solid lines are Gaussian fits (for clarity, the spectra are shifted). In comparison to fig. 5.10, the QDs affect the slope of the Urbach tail in the opposite way. Accentuating a further difference, the center energy of the peaks of sample D clearly deviates pointing to a movement of the GaAs band gap energy

The shift of the peak energy of the SI-GaAs derivatives in fig. 5.12 is caused by the different thicknesses of the used substrates ( $533 \mu\text{m}$  and  $350 \mu\text{m}$  for sample B and D, respectively), whereas the distinct peak displacement of sample D indicates an influence of the QDs on the GaAs energy band gap. Consequently, aside from the impact on the Urbach tail, it seems QD dispersion on GaAs can be used to alter the band gap energy of the wafer.

## Conclusions

By observation of photoinduced doping effects in the PL of colloidal PbS QDs, the work demonstrates the close relationship between superlattices and QD ensembles. Most notably, optically stimulated QD arrays respond as a collective as expected from bulk samples. In the meantime, we confirmed dynamic three-dimensional band filling in 4.7 nm PbS QDs as well [32]. Summarizing the results of the absorbance measurements, it is demonstrated that - independent of the ambient temperature - size reduction below 3 nm bleaches the acoustic phonon branch in lead-salt QDs. Consequently, the thermally induced shift of the OA spectra is practically ruled by the coupling to optical phonons only and, therefore, the  $E_g$  trend barely displays nonlinearity at cryogenic temperatures. The phenomenon can be considered as inherent lattice cooling in strongly confined matter and emphasizes the potential of strongly size-quantized semiconductors to be used for the fabrication of intense light emitters with stable, temperature invariant chromaticity. Finally, we address here the impact of PbS QDs on the absorption properties of GaAs. Employing TR spectroscopy, we observe the Urbach tail slope changes of the GaAs absorption edge due to the presence PbS QDs. The size of the latter can be used to enhance or to weaken the below-band gap absorption of the GaAs substrates. The findings give new

insights in optical device engineering using either charge transfer between bulk and quantized matter, interfacial impurities between QDs and bulk, bleaching of vibronic modes, or the superposition of individual absorption spectra in order to tune the slope of the absorption edge or to alter the energy band gap itself.

## Acknowledgement

The work was supported by the DGAPA-UNAM PAPIIT project TB100213-RR170213 (PI Bruno Ullrich). B U and A K S acknowledge the DGAPA-UNAM program of post-doctoral scholarships.

## References

1. Singh J. Optoelectronics. Singapore: McGraw-Hill; 1996.
2. Schubert E F. Doping in III-V semiconductors. New York: Cambridge; 1993.
3. Ullrich B, Zhang C, Fronius H, v Klitzing K. Photocurrent spectroscopy in a sawtooth doping superlattice. *Applied Physics Letters* 1988; 52(23) 1967-1969.
4. Schubert E F, Stark J, Ullrich B, Cunningham J E. Spatial localization of impurities in  $\delta$ -doped GaAs. *Applied Physics Letters* 1988; 52(18) 1508-1510.
5. Ullrich B, Zhang C, Schubert E F, Cunningham J E, v Klitzing K. Transmission spectroscopy on sawtooth-doping superlattices. *Physical Review B* 1989; 39(6) 3776-3779.
6. Brus L. Quantum crystallites and nonlinear optics. *Applied Physics A* 1991; 53 465-474.
7. Grundmann M. The Physics of semiconductors. Berlin: Springer; 2006.
8. Schroeder R, Ullrich B. Photovoltaic hybrid device with broad tunable spectral response achieved by organic/inorganic thin-film heteropairing. *Applied Physics Letters* 2002; 81(3) 556-558.
9. Wang J S, Ullrich B, Brown G J, Wai C M. Morphology and energy transfer in PbS quantum dot arrays formed with supercritical fluid deposition. *Materials Chemistry and Physics* 2013; 141 195-202.
10. Ullrich B, Wang J S, Brown G J. Analysis of thermal band gap variations of PbS quantum dots by Fourier transform transmission and emission spectroscopy. *Applied Physics Letters* 2011; 99 081901 3 pp.
11. Ullrich B, Brown G J. Note: Phase sensitive detection of photoluminescence with Fourier transform spectroscopy. *Review of Scientific Instruments* 2012; 83 016105 3 pp.
12. Ullrich B, Wang J S, Xiao X Y, Brown G J. Fourier spectroscopy on PbS quantum dots. *SPIE Proceedings* 2012; 8271 82710A 6 pp.
13. Moss T S, Burrell G J, Ellis B. Semiconductor opto-electronics. New York: John Wiley & Sons; 1973.
14. Kamat V, Dimitrijevic N M, Nozik A J. Dynamic Burstein-Moss shift in semiconductor colloids. *The Journal of Physical Chemistry* 1989; 93 2873-2875.
15. Ullrich B, Wang J S. Impact of laser excitation variations on the photoluminescence of PbS quantum dots on GaAs. *Journal of Luminescence* 2013; 143 645-648.
16. Ullrich B, Wang J S. All-optical tuning of the Stokes shift in PbS quantum dots. *Applied Physics Letters* 2013; 102 071905 3 pp.

17. Hens Z, Moreels I. Light absorption by colloidal semiconductor quantum dots. *Journal of Materials Chemistry* 2012; 22 10406-10415.
18. Yue F, Tomm J W, Kruschke D. Spontaneous and stimulated emission dynamics of PbS quantum dots in a glass matrix. *Physical Review B* 2013; 87 195314 13 pp.
19. Liptay T J, Ram R J. Temperature dependence of the exciton transition in semiconductor quantum dots. *Applied Physics Letters* 2006; 89 223132 3 pp.
20. Konstantatos G, Sargent E H., editors. *Colloidal quantum dot optoelectronics and photovoltaics*. New York: Cambridge; 2013.
21. Moreels I, Lambert K, Smeets D, De Muynck D, Nollet T, Martins J C, Vanhaecke F, Vantomme A, Delerue C, Guy A, Hens Z. Size-dependent optical properties of colloidal PbS quantum dots. *ACS Nano* 2009; 3(10) 3023-3030.
22. Ullrich B, Xiao X Y, Brown G J. Photoluminescence of PbS quantum dots on semi-insulating GaAs. *Journal of Applied Physics* 2010; 108 013525 5 pp.
23. Hall R N. Recombination processes in semiconductors. *Proceedings of the IEE - Part B: Electronic and Communication Engineering* 1959; 106(17S) 923 – 931.
24. Ullrich B, Antillón A, Bhowmick M, Wang J S, Xi H. Atomic transition region at the crossover between quantum dots to molecules. *Physica Scripta* 2014; 89 025801 4 pp.
25. Zhang J, Jiang X. Confinement-dependent below-gap state in PbS quantum dot films probed by continuous-wave photoinduced absorption. *The Journal of Physical Chemistry B* 2008; 112, 9557-9560.
26. Fan H Y. Temperature dependence of the energy gap in semiconductors. *Physical Review* 1951; 82, 900-905.
27. Ullrich B, Ariza-Flores D, Bhowmick M. Intrinsic photoluminescence Stokes shift in semiconductors demonstrated by thin-film CdS formed with pulsed-laser deposition. *Thin Solid Films* 2014; 558 24-26.
28. Rossetti R, Hull R, Gibson J M, Brus L E. Hybrid electronic properties between the molecular and solid state limits: Lead sulfide and silver halide crystallinities. *The Journal of Chemical Physics* 1985; 83 1406-1410.
29. Olkhovets A, Hsu R-C, Lipovskii A, Wise F W. Size-dependent temperature variation of the energy gap in lead-salt quantum dots. *Physical Review Letters* 1998; 16 3539-3542.
30. Bleicher M. *Halbleiter-Optoelektronik*. Heidelberg: Huethig; 1985.
31. Abel K A, Shan J, Boyer J-C, Harris F, van Veggel F C J M. Highly photoluminescent PbS nanocrystals: The beneficial effect of trioctylphosphine. *Chemistry of Materials* 2008; 20(12) 3794-3796.
32. Ullrich B, Xi H, Wang J S. Photoinduced band filling in strongly confined colloidal PbS quantum dots. *Journal of Applied Physics* 2014; 115 233503 4 pp.